

UDC 548.737:543.422

**MOLECULAR AND CRYSTAL STRUCTURE, SPECTROSCOPIC PROPERTIES
OF 2-METHYL-4-(3-METHYL-3-PHENYL-CYCLOBUTYL)-THIAZOLE DETERMINED
BY THE EXPERIMENTAL METHOD AND A QUANTUM CHEMICAL CALCULATION**

© 2012 C. Yüksektepe^{1*}, N. Çalışkan², I. Yılmaz³, A. Çukurovalı⁴

¹Department of Physics, Faculty of Science, Cankiri Karatekin University, 18100-Ballica, Cankiri, Turkey

²Department of Physics, Faculty of Arts and Sciences, Ondokuz Mayıs University, 55139-Kurupelit, Samsun, Turkey

³Department of Chemistry, Faculty of Science, Karamanoglu MehmetBey University, 70100-Karaman, Turkey

⁴Department of Chemistry, Faculty of Science, Firat University, 23119-Elazig, Turkey

Received December, 14, 2010

The structure of the synthesized title compound is characterized by IR, UV-Visible spectroscopy, and single-crystal X-ray diffraction (XRD). The new compound ($C_{18}H_{23}NS$) crystallizes in the monoclinic $P2_1/c$ space group. In addition to the crystal structure from the X-ray experiment, the molecular geometry, vibrational frequencies, atomic charge distribution, and frontier molecular orbital (FMO) analysis of the title compound in the ground state are calculated by density functional theory (B3LYP) with 6-311G(*d,p*) and 6-31G(*d,p*) basis sets. The results of the optimized molecular structure are presented and compared with the experimental values. The computed vibrational frequencies are used to determine the types of molecular motions associated with each of the observed experimental bands. To determine the conformational flexibility, the molecular energy profile of (1) is obtained by semi-empirical (AM1) and (PM3) calculations with respect to a selected degree of torsional freedom. Moreover, molecular electrostatic potential (MEP) and thermodynamic parameters of the title compound were calculated by the theoretical methods.

К e y w o r d s: *ab initio* calculation, semi-empirical method, B3LYP, conformational analysis, vibrational assignment, X-ray structure determination.

INTRODUCTION

Benzothiazolium groups have been used in organic dyes as either electron withdrawing or electron donating substituents, depending on whether the N atom is cationic or not [1]. Various thiazole derivatives show herbicidal, anti-inflammatory, antimicrobial, and antiparasite activity [2, 3] and also liquid crystal properties [4].

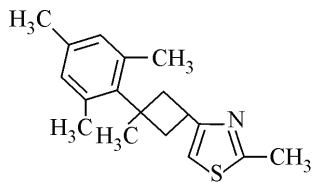
The aim of this work is to describe and investigate the molecular and crystal structure of the new synthesized compound by a complex of physical and chemical methods, including IR and UV spectroscopy and X-ray single crystal analysis and *ab initio* quantum chemical calculations of the compound with the formula $C_{18}H_{23}NS$. A number of papers have recently appeared in the literature concerning the calculation of vibrational assignments by quantum chemistry methods [5—9]. This papers indicate that geometry optimization is a crucial factor in an accurate determination of computed vibrational frequencies. Moreover, it is known that the DFT (B3LYP) method adequately takes into account electron correlation contributions that are especially important in systems containing extensive electron conjugation and/or electron lone pairs. However, considering that as the molecular size increases, computing time also increases. The DFT level was used to optimize computing time.

* E-mail: yuksekc@yahoo.com, yuksektepe.c@karatekin.edu.tr

In this study, we present the results of a detailed investigation of the synthesis and structural characterization of 2-methyl-4-(3-methyl-3-phenyl-cyclobutyl)-thiazole using single crystal X-ray, IR, UV spectroscopy and quantum chemical methods. Vibrational assignments, Mulliken atomic charges, thermodynamic parameters, and frontier molecular orbital (FMO) analysis of the title compound in the ground state have been calculated using the DFT(B3LYP) methods with 6-311G** (where ** is shown (*d,p*)) and 6-31G** basis sets. A comparison of the experimental and theoretical spectra can be very useful in making correct assignments and understanding the molecular structure relationship. And so, these calculations are valuable for providing insight into molecular analysis.

EXPERIMENTAL

Synthesis of the 2-methyl-4-(3-methyl-3-phenyl-cyclobutyl)-thiazole compound. IR spectra of the compound were recorded in the range of 4000—450 cm⁻¹ with a Mattson 1000 FT-infrared spectrometer using KBr pellets. The compound was synthesized as in Scheme 1 by the following procedure. To a solution of thioacetamide (0.7513 g, 10 mmol) in 50 ml of absolute benzene, a solution of 1-methyl-1-mesityl-3-(2-chloro-1-oxoethyl) cyclobutane (2.6479 g, 10 mmol) in 20 ml of absolute benzene was added. After the addition of the halo ketone, the temperature was raised to 323—328 K and kept at this temperature for 2 h. The solvent was removed under reduced pressure and the obtained residue was treated with water and then made alkaline with an aqueous solution of NH₃ (5%). A white precipitate was separated by suction, washed with an aqueous NH₃ solution several times, and dried in air. Single crystals suitable for crystal structure determination were obtained by slow evaporation of its ethanol solution. Yield: 63 %, melting point: 373 K.



Measurement. IR spectra were recorded on an ATI Unicam-Mattson 1000 FT-IR spectrophotometer using KBr pellets. The UV spectra of the compound were measured on a Schimadzu UV-1700 spectrometer in the CHCl₃ solvent.

X-ray crystallography. The data collection was performed at 293 K on a Stoe-IPDS-2 diffractometer with graphite monochromated MoK_α radiation ($\lambda = 0.71073 \text{ \AA}$). The structure was solved by direct methods using SHELXS-97 and refined by a full-matrix least-squares procedure using the SHELXL-97 program [10]. All non-hydrogen atoms were easily found from the difference Fourier map and refined anisotropically. All hydrogen atoms were included using a riding model and refined isotropically with C—H = 0.93—0.97 Å and N—H = 0.86 Å. $U_{\text{iso}}(\text{H}) = 1.2U_{\text{eq}}(\text{C, N})$, $U_{\text{iso}}(\text{H}) = 1.5U_{\text{eq}}$ (for the methyl group).

CALCULATION DETAILS

Theoretical calculations were carried out using semi-empirical AM1, PM3, and *ab initio* DFT B3LYP/6-311G** and B3LYP/6-31G** quantum chemical methods [11—13]. For modeling, the experimental data were supplemented using the semi-empirical and *ab initio* quantum chemical calculations. The molecular geometry is restricted and all the calculations are performed without specifying any symmetry for the title molecule using the Gaussian 03 Program package [14] on a personal computer. Then the vibrational frequencies for the optimized molecular structures were calculated. No scale factor was used in the calculated frequencies. The Gauss-View Molecular Visualization program was used to assign the calculated harmonic frequencies [15]. To identify low-energy conformations, selected degrees of torsional freedom, $T(\text{C13—C10—C1—C6})$, were varied from -180° to $+180^\circ$ in steps of 10° , and the molecular energy profile was obtained at the semi-empirical AM1 and PM3 levels.

Table 1

Crystallographic data of (1)

Empirical formula	C ₁₈ H ₂₃ NS
Molecular weight	285.5
Temperature, T, K	296
Wavelength, Å	0.71073
Crystal system	Monoclinic
Crystal size, mm ³	0.640×0.540×0.470
Space group	P2 ₁ /c
a, b, c, Å	11.1064(4), 8.0100(2), 21.0825(8)
α, β, γ, deg.	90, 119.015(3), 90
Volume, V, Å ³	1640.15(31)
Z	4
T _{min} , T _{max}	0.9057, 0.9467
Calculated density, mg/cm ³	1.16
θ range deg.	2.1—25.0
Index ranges	h = -13→13, k = -9→9, l = -24→24
Measured reflections	20366
Independent reflections	2890
Observed reflections (I > 2σ)	2481
Goodness-of-fit on F ²	1.066
R1 indices (I > 2σ)	0.039
wR2 indices (I > 2σ)	0.105

RESULTS AND DISCUSSION

Crystal structure. Details of crystal parameters, data collection, structure solution and refinement are given in Table 1. An ORTEP-3 [16] drawing of the title compound with the atom labeling scheme is shown in Fig. 1. The title compound (1) contains phenyl, cyclobutane, and thiazole moieties. The central five-membered thiazole ring is essentially planar, to within 0.0030 Å. The dihedral angles between the phenyl and cyclobutane rings with the thiazole ring are 85.77(06)° and 89.08(08)° respectively. Only some of bond distances in the thiazole ring show a partial double bond character so that C15—N1, S1—C16, and S1—C17 bond distances of 1.380(2), 1.706(2), 1.719(2) Å show the values of a single bond character (Table 2). The S—C bond distances are shorter than the accepted value for an S—C(sp²) single bond of 1.76 Å [17]. It is worth noting that the C17—N1 bond distance value of 1.300(2) Å falls into the C=N double bond distance region and is shorter than the C=N double bond distance found in a related thiazole ring structure [18]. Also in the thiazole ring, the C12—C13 bond distance of 1.341(2) Å shows the value of the C=C double bond character.

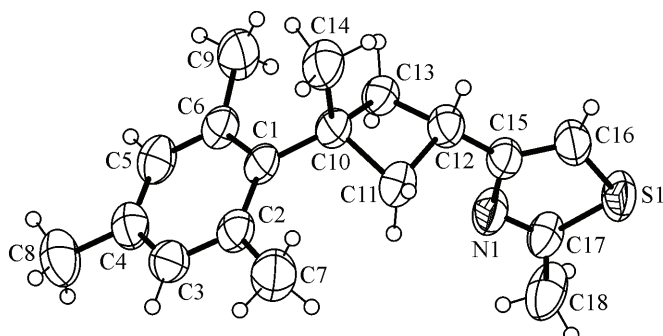


Fig. 1. Experimental geometric structure of the title compound

Table 2

Optimized and experimental geometric parameters of the title compound in the ground state

Atoms	Experi- mental	B3LYP 6-311G**	B3LYP 6-31G**	Atoms	Experi- mental	B3LYP 6-311G**	B3LYP 6-31G**
Bond lengths (Å)							
S1—C16	1.706(2)	1.736	1.737	N1—C17	1.300(2)	1.296	1.300
S1—C17	1.719(2)	1.763	1.766	C15—C16	1.341(2)	1.364	1.367
N1—C15	1.380(2)	1.383	1.386				
Bond angles (deg.)							
C15—N1—C17	111.02(15)	112.57	112.27	N1—C17—C18	124.27(18)	124.49	124.40
N1—C15—C16	114.72(16)	114.54	114.69	S1—C17—C18	121.49(15)	121.88	121.81
Torsion angles (deg.)							
C15—N1—C17—C18	177.6(2)	179.93	179.94	C12—C15—N1—C17	-175.4 (2)	-179.99	-180.00
C16—S1—C17—C18	-178.0(2)	-179.93	-179.94	C12—C15—C16—S1	175.1(2)	179.99	179.99

The steric interaction between the substituent groups on the cyclobutane ring means that this ring deviates significantly from planarity. Literature values for the puckering of the cyclobutane ring are 29.03(13)° in [19] and 26.8(2)° in [20]. In this paper, the C13/C10/C11 plane forms a dihedral angle of 23.49(13)° with the C13/C12/C11 plane. In the crystal packing there is no classic hydrogen bond, however, there are π...ring interaction effects. The C8 atom of the methyl group at (*x*, *y*, *z*) acts as a donor to centroid the thiazole ring (*Cg*2) at (2-*x*, 1/2+*y*, 1/2-*z*, H...*Cg* = 2.65 Å and D—H...*Cg* = = 155°). Eventually, the adjacent molecules are linked to each other by the C—H...π interaction into a chain running along the *b* axis of the monoclinic cell (Fig. 2).

FT—IR spectroscopy. The vibrational frequencies are calculated at the B3LYP/6-311G** and B3LYP/6-31G** levels. Some primary calculated harmonic frequencies are listed in Table 3 and compared with the experimental data. As seen from Table 3, the predicted vibrational frequencies are consistent with those from the experimental results.

Our calculations of the title compound are compared to the experimental results. The characteristic ν(CH) stretching vibrations of heteroaromatic structures are expected to appear in 3000—3100 cm⁻¹ frequency ranges [21, 22]. In the present study, four ν(CH) stretching vibrations of the title compound are observed experimentally, as shown in Table 3. The highest normal mode of vibration corresponds to the ν(CH) stretching in the thiazole ring, which is calculated at 3267 cm⁻¹ for the B3LYP/6-31G** method. In thiazole, the ν(C—N) and ν(C=N) stretching modes were observed to be 1319 cm⁻¹ and 1531 cm⁻¹ as experimentally, and 1311 cm⁻¹ and 1522 cm⁻¹ for the B3LYP/6-31G* level, and 1321 cm⁻¹ and 1547 cm⁻¹ for the HF/6-31G* level [6]. Here this modes are found to be 1309 cm⁻¹ and 1526 cm⁻¹ as experimentally; 1334 cm⁻¹ and 1578 cm⁻¹ for the B3LYP/6-311G** level; 1344 cm⁻¹ and 1591 cm⁻¹ for the B3LYP/6-31G**

Fig. 2. Part of the crystal structure of the title molecule, showing the formation of a chain; the *b* axis of the monoclinic cell. For clarity, only H atoms involved in hydrogen bonding have been included

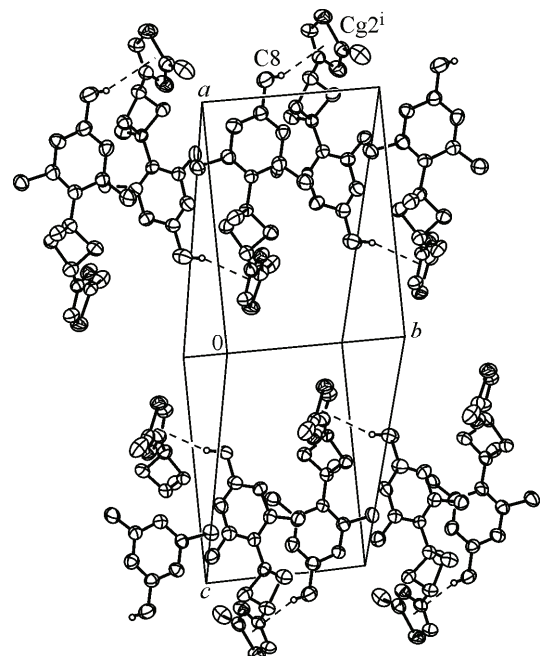


Table 3

Comparison of the observed and calculated vibrational spectra of the title compound

Frequencies	Experimental	B3LYP 6-311G**	B3LYP 6-31G**
$\nu(\text{CH})$ thi.	3226	3246	3267
$\nu_s(\text{CH})$ phe.	3134	3145	3162
$\nu_{\text{as}}(\text{CH})$ phe.	3127	3143	3160
$\nu_{\text{as}}(\text{CH}_3)$ thi.	3104	3132	3155
$\nu_{\text{as}}(\text{CH}_2)$	3074	3123	3141
$\nu_{\text{as}}(\text{CH}_3)$ phe.	3064	3091/3071	3129/3034
$\nu_{\text{as}}(\text{CH}_3)$ cycl.	3027	3082	3113
$\nu(\text{CH})$ cycl	3005	3064	3078
$\nu_s(\text{CH}_2)$	2970	3052	3068
$\nu_s(\text{CH}_3)$ phe.	2960	3037/3018	3052
$\nu_s(\text{CH}_3)$ thi.	2933	3034	3050
$\nu_s(\text{CH}_3)$ cycl.	2862	3020	3037
$\nu(\text{CC})$ phe.	1609	1649	1664
$\nu(\text{C} = \text{N}) + \nu(\text{C} = \text{C})$ thi.	1526	1578	1591
$\rho_s(\text{CH}_3)$ phe.	1482	1521	1531
$\rho_s(\text{CH}_3)$ cycl.	1459	1507	1517
$\rho_s(\text{CH}_2)$	1444	1492	1502
$\rho_s(\text{CH}_3)$ thi.	1430	1487	1489
$w(\text{CH}_3)$	1376	1408	1420
$\delta(\text{CH})$ cycl.+thi.	1365	1374	1379
$\nu(\text{CN})$	1309	1334	1344
$\theta(\text{Ring}) + w(\text{CH}_2)$	1289	1300	1306
$\rho_r(\text{CH})$ phe.	1208	1218	1286
$\nu(\text{CC}) + \delta(\text{CH})$ cycl.+thi.	1182	1192	1199
$\rho_r(\text{CH}_3)$	1073	1089	1092
$t(\text{CH}_2)$	1030	1073	1077
$\delta(\text{CNC})$	977	991	994
$t(\text{CH})$ phe.	856	893	896
$w(\text{CH})$ phe.	780	869	874
$\nu(\text{CS})$	742	851	857
$\gamma(\text{CH})$ thi.	670	713	752
$\delta(\text{CSC})$	583	586	587

thi: thiazole, phe: phenyl, cycl: cyclobutane, ν : stretching, ν_s : symmetric stretching, ν_{as} : asymmetric stretching, δ : bending, ρ_r : rocking, t : twisting, ρ_s : scissoring, w : wagging, θ : breathing.

level. These results indicated some band shifts with regard to the different-substituent thiazole ring. On the other hand, the CH_3 asymmetric and symmetric stretching frequencies are observed experimentally and also calculated theoretically. All these results are in good agreement with the literature values [21, 23, 24]. Other essential characteristic vibrations of the title compound as rocking, bending, scissoring, out-of-plane bending, wagging, twisting, breathing are compared in Table 3. As seen, the experimental frequency values are in good agreement with the frequencies calculated by B3LYP methods.

Theoretical structure. We noted that the experimental results belong to the solid phase and the theoretical calculations belong to the gaseous phase. In the solid state, the existence of the crystal field along with intermolecular interactions have connected the molecules together, which results in the differences of bond parameters between the calculated and experimental values. Some selected geometric parameters are listed in Table 2, and the theoretical values are compared with the X-ray experimental data. This calculated geometric parameters generally give bond lengths that are slightly larger than the experimental values. The largest differences between the experimental and calculated bond lengths, bond and torsion angles are 0.044 Å and 0.047 Å, 1.50°, and 1.25°, 4.89° and 4.89° for B3LYP/6-311G** and B3LYP/6-31G** respectively. The considerable differences between the calculated and experimental data on the bond lengths and bond angles correspond to the SC bond, CNC dihedral and CCCS torsion angles. As a result, the optimized bond lengths obtained by the B3LYP/6-311G** method and dihedral angles obtained by the B3LYP/6-31G** method show the best agreement with the experimental values.

Conformational analysis. Based on the B3LYP/6-311G** and B3LYP/6-31G** optimized geometry, the total energy of the title compound has been calculated by these two methods and the values are -1152.908 a.u. and -1152.731 a.u. respectively. In order to define the preferential position of the benzene ring with respect to the cyclobutane ring, a preliminary search of low-energy structures was performed using AM1 and PM3 computations as a function of the selected degree of torsional freedom $T(\text{C13}-\text{C10}-\text{C1}-\text{C6})$. According to the X-ray crystallographic study, the $T(\text{C13}-\text{C10}-\text{C1}-\text{C6})$ torsion angle is -42.1(2)°; the same torsion angle is observed as -40.866°, -40.905°, -40.000°, and -44.860° in the B3LYP/6-311G**, B3LYP/6-31G**, AM1, and PM3 optimized geometry of the title compound respectively.

The energy profile as a function of $T(\text{C13}-\text{C10}-\text{C1}-\text{C6})$ shows two maxima at -130° and 50° and two minima at -40° and 140°, having an energy of 45.089 kcal·mol⁻¹ and 45.110 kcal·mol⁻¹ for AM1, while this torsion angle shows four maxima at -150°, -110°, 30°, and 70° and two minima at -40° and 140°, having an energy of 31.921 kcal·mol⁻¹ and 31.749 kcal·mol⁻¹ for the PM3 method (Figs. 3 and 4). The energy difference between the heat of formation values of the most favorable and unfavorable conformer, which arises from the rotational potential barrier calculated with respect to the selected torsion angle, is calculated as 12.189 kcal·mol⁻¹ and 10.188 kcal·mol⁻¹ for AM1 and PM3 respectively. The AM1 and PM3 optimized geometries of the crystal structure of the title compound, corresponding to the non-planar conformation, are the most stable conformations, which agrees with the result obtained from the X-ray investigation.

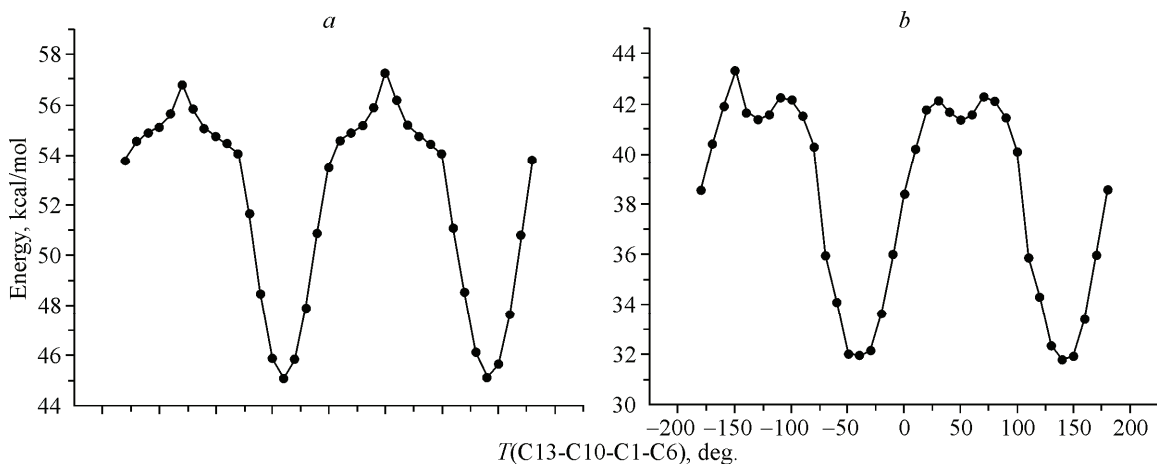


Fig. 3. Molecular energy profile against the selected torsional degree $T(\text{C13}-\text{C10}-\text{C1}-\text{C6})$ of freedom for the AM1 method (a), PM3 method (b)

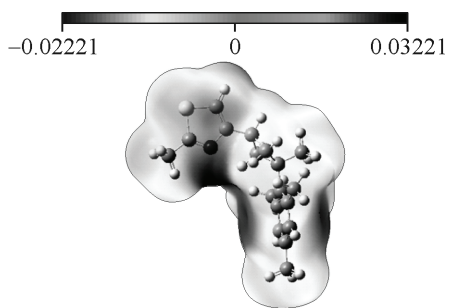


Fig. 4. Molecular electrostatic potential map of the title compound

computational results that the most stable conformer of the title compound is principally determined by the non-bonded torsional energy term affected by packing of the molecules.

The Mulliken atomic charges of the title compound were calculated at B3LYP/6-311G**, B3LYP/6-31G** levels and illustrated in Table 4. Atomic charge analysis revealed that charge distributions of the N1 atom and the sum of atomic charges in phenyl (Cg(3)) and thiazole (Cg(2)) rings are -0.31 , -0.33 , and 0.12 for the B3LYP/6-311G** level respectively. The calculated results show that the N atom has a bigger negative charge than some of the other atoms. In addition, the calculated atomic charge of the C8 atom is also -0.26 . The atomic charge analysis shows that the C8 atom behaves as a strong donor in the intermolecular C8—H8B...Cg(2) interaction, and also there is a Cg...Cg (face-to-face) interaction between the Cg(2) and Cg(3) ring centroids.

Molecular electrostatic potential. The molecular electrostatic potential (MEP) is related to the electron density and is a very useful descriptor to determine sites for electrophilic attack and nucleophilic reactions as well as hydrogen bonding interactions [26—28]. The electrostatic potential $V(r)$ is also well suited for analyzing processes based on the recognition of one molecule by another, as in drug—receptor and enzyme—substrate interactions, because it is through their potentials that the two species first "see" each other [29, 30]. Being a real physical property, $V(r)$ can be determined experimentally by diffraction or computational methods [31].

To predict reactive sites for electrophilic and nucleophilic attack for the title molecule, MEP was calculated at the B3LYP/6-311G** optimized geometry. The negative regions of MEP were related to electrophilic reactivity and the positive regions to nucleophilic reactivity shown in Fig. 5. As can be seen from the figure, there is a possible site on the title compound for electrophilic attack. The negative region is located on the unprotonated nitrogen atom of the thiazole ring, N1 around the phenyl ring, with a maximum value of -0.02221 a.u. However, the maximum positive region is located on the methyl group, probably due to hydrogen, with a maximum value of 0.03221 a.u. This results provide information concerning the region where the compound can interact intermolecularly and bond metallically. Therefore, Fig. 5 confirms the existence of the intermolecular C8—H8B...Cg(2) interaction.

Table 4

*Mulliken atomic charges of the title compound at the B3LYP/6-311G** and B3LYP/6-31G** levels*

Atoms	B3LYP 6-311G**	B3LYP 6-31G**	Atoms	B3LYP 6-311G**	B3LYP 6-31G**
C1	0.03	0.04	C11	-0.09	-0.17
C2	-0.08	0.09	C12	-0.23	-0.15
C3	-0.05	-0.17	C13	-0.09	-0.17
C4	-0.10	0.14	C14	-0.18	-0.31
C5	-0.05	-0.17	C15	0.17	0.31
C6	-0.08	0.09	C16	-0.30	-0.34
C7	-0.26	-0.37	S1	0.22	0.21
C8	-0.26	-0.38	C17	-0.06	0.09
C9	-0.26	-0.37	N1	-0.31	-0.45
C10	-0.35	-0.05	C18	-0.26	-0.37

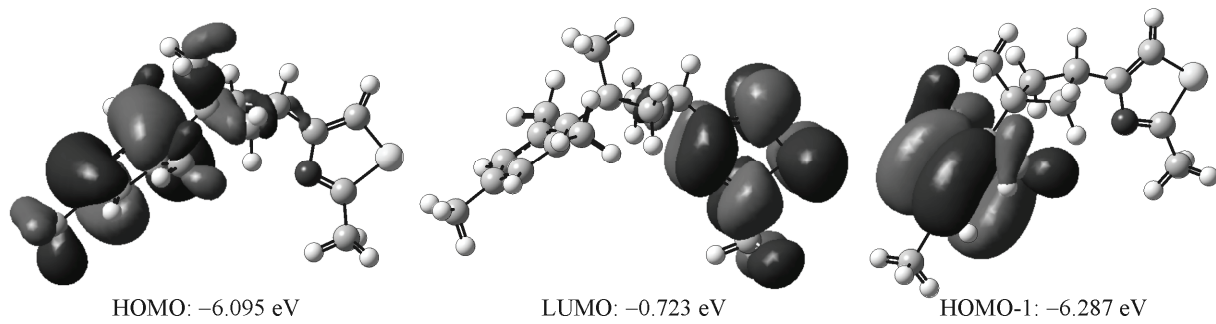


Fig. 5. Molecular orbital surfaces and given energy levels for HOMO-1, HOMO, and LUMO of the title compound computed at the B3LYP/6-311G** level

Frontier molecular orbital analysis. Fig. 5 shows the distributions and energy levels of HOMO-1, HOMO, and LUMO computed at the B3LYP/6-311G** level for the title compound. The calculations indicate that the compound has 89 occupied molecular orbitals (MOs). The highest occupied molecular orbital (HOMO) and the lowest unoccupied molecular orbital (LUMO), energy gaps, and total energies for the mentioned molecule were calculated and are given in Table 5. An electronic system with a larger HOMO-LUMO gap should be less reactive than the one having a smaller gap [32]. The differences between HOMO and LUMO energy values of the molecule are 5.372 eV, 5.390 eV for B3LYP/6-311G** and B3LYP/6-31G** methods respectively, as seen in Table 5. The absorption peaks are experimentally observed at 239 nm and 226 nm for the title compound. It can be seen that these peaks correspond to $n \rightarrow \pi^*$ and $\pi \rightarrow \pi^*$ transitions. Electron transfer (ET) peaks for the B3LYP/6-311G** and B3LYP/6-31G** levels are theoretically at 232 nm, 224 nm and 231 nm, 223 nm to correspond to the UV-Vis spectral absorption peaks, and the corresponding electron transfers happened between HOMO and LUMO, HOMO-1 and LUMO respectively. The larger theoretical absorption wavelengths of the compound have slight blue-shifts comparing with the corresponding experimental ones.

Table 5

Frontier molecular orbitals of the title compound

Energies	B3LYP 6-311G**	B3LYP 6-31G**	Energies	B3LYP 6-311G**	B3LYP 6-31G**
HOMO (a.u.)	-0.224	-0.216	Δ (a.u.) (eV)	0.197 (5.372)	0.198 (5.390)
LUMO (a.u.)	-0.027	-0.018	HOMO-1 (a.u.)	-0.231	-0.223

Table 6

Calculated energies (a.u), zero-point vibrational energies (kcal·mol⁻¹), rotational constants (GHz), entropies and heat capacities (ca·mol⁻¹·K⁻¹), and dipole moment (D) for the title compound

Parameters	B3LYP 6-311G**	B3LYP 6-31G**	Parameters	B3LYP 6-311G**	B3LYP 6-31G**
Total energy (a.u.)	-1152.908	-1152.731			
Dipole moment (D)	0.9472	0.8258	Translational	42.842	42.842
Zero-point vib. energy	228.823	230.231	Rotational	34.529	34.536
Rotational constants	0.57062	0.57429	Vibrational	74.802	73.891
	0.15109	0.14984	Total	152.172	151.269
	0.14195	0.14112			
			Heat capacity (C_v)		
Translational	2.981	2.981	Vibrational	73.369	73.029
Rotational	2.981	2.981	Total	79.331	78.991

Thermodynamic parameters of the title compound. Several thermodynamic parameters have been calculated using B3LYP/6-311G** and B3LYP/6-31G** levels as and are given in Table 6. The total energies, zero-point vibrational energy (ZPVE), entropy ($S_{\text{vib}}(T)$), and heat capacity ($C_{\text{vib}}(T)$) of the title compound at 298.15 K temperature and 1 atm pressure obtained with different basis sets and theoretical methods are also presented. ZPVE obtained by the B3LYP/6-311G** method is much lower than that obtained by the B3LYP/6-31G** method. They are $228.823 \text{ kcal}\cdot\text{mol}^{-1}$ and $230.231 \text{ kcal}\cdot\text{mol}^{-1}$ by B3LYP/6-311G** and B3LYP/6-31G** respectively. The dipole moment obtained at the B3LYP/6-311G** level is the highest one (0.9472 D), and the value obtained at the B3LYP/6-31G** level is 0.8258. Therefore, the results of the energies, dipole moment, entropy, heat capacity, and ZPVE can be useful to the new synthesis of some molecules that include the thiazole core.

CONCLUSIONS

In this study, to test the DFT level with different basis sets reported, the computed and experimental geometric parameters, vibrational frequencies, and frontier molecular orbitals of the title compound have been compared. Furthermore, the analysis of the low-energy structures was performed using AM1 and PM3 computations as a function of the selected degree of torsional freedom $T(\text{C}13-\text{C}10-\text{C}1-\text{C}6)$ and several thermodynamic parameters. To fit the theoretical frequency, frontier molecular orbitals, ZPVE, entropy, and heat capacity results with the experimental ones for the B3LYP levels, we have multiplied the data. The multiplication factor results gained seemed to be in good agreement with experimental ones. The B3LYP levels that include the effects of electron correlation have shown good fit to the experimental ones in terms of geometric parameters, vibrational frequencies, and MO energies. Despite the differences observed in the geometric parameters, the general agreement is good, and the theoretical calculations support the solid state structures. Moreover, crystal packing of the title compound is dominated only by intermolecular C—H... π interactions formed during the preparation or crystallization. These interactions supply the leading contribution to the stability and crystal structure order and are presumably responsible for the discrepancies between the experimental and calculated structures.

Supplementary Material. Crystallographic data for the structural analysis have been deposited with the Cambridge Crystallographic Data Centre, CCDC No 748349. Copies of this information may be obtained free of charge from the Director, CCDC, 12 Union Road, Cambridge CB2 1EZ, UK (fax: +44-1223-336033; e-mail: deposit@ccdc.cam.ac.uk or www: <http://www.ccdc.cam.ac.uk>).

Acknowledgements. The authors wish to acknowledge the Faculty of Arts and Sciences, Ondokuz Mayıs University, Turkey, for the use of the STOE IPDS-II diffractometer (purchased under grant F.279 of the University Research Fund).

REFERENCES

1. Zollinger H., Colour Chemistry Syntheses Properties and Applications of Organic Dyes and Pigments 2nd ed Weinheim: VCH, 1991.
2. Koparır M., Cansız A., Ahmedzade M. et al. // Heteroat. Chem. – 2004. – **15**. – P. 26. – 31.
3. Ahmedzade M., Çukurovalı A., Koparır M. // J. Chem. Soc. Pak. – 2003. – **25**. – P. 51. – 53.
4. Coghi L., Lanfredi A.M.M., Tripicchio A. // J. Chem. Soc. Perkin. Trans. – 1976. – **2**. – P. 1808. – 1810.
5. Dinçer M., Avcı D., Şekerci M. et al. // J. Mol. Model. – 2008. – **14**. – P. 823. – 832.
6. Özdemir N., Dinçer M., Çukurovalı A. et al. // J. Mol. Model. – 2009. – **15**. – P. 1435. – 1445.
7. Misra N., Prasad O., Sinha L. et al. // J. Mol. Struct. (Theochem). – 2007. – **822**. – P. 45. – 47.
8. Jian F., Zhao P., Guo H. et al. // Spectrochim. Acta. – 2008. – **A69**. – P. 647. – 653.
9. Choo J., Yoo S., Moon S. et al. // Vibr. Spectr. – 1998. – **17**. – P. 173. – 182.
10. Sheldrick G.M. SHELXS-97 and SHELXL-97, Germany, University of Gottingen, 1997.
11. Lee C., Yang W., Parr R.G. // Phys. Rev. – 1988. – **B37**. – P. 785. – 789.
12. Becke A.D. // J. Chem. Phys. – 1993. – **98**. – P. 5648. – 5652.
13. Ditchfield R., Hehre W.J., Pople J.A. // J. Chem. Phys. – 1971. – **54**. – P. 724. – 728.

14. Frisch M.J., Trucks G.W., Schlegel H.B. et al. Gaussian 03. Revision E.01. Gaussian Inc., Wallingford, CT, 2004.
15. Dennington R.I.I., Keith T., Millam J. GaussView, Version 4.1.2. Semichem Inc, Shawnee Mission, KS, 2007.
16. Farrugia L.J. // J. Appl. Crystallogr. – 1997. – **30**. – P. 565. – 566.
17. Allen F.H. // Acta Crystallogr. – 1984. – **B40**. – P. 64. – 72.
18. Yüksektepe Ç., Çalışkan N., Yılmaz I. et al. // Acta Crystallogr. – 2006. – **E62**. – P. o2762. – o2764.
19. Yüksektepe Ç., Saracoğlu H., Koca M. et al. // Acta Crystallogr. – 2004. – **C60**. – P. o509. – o510.
20. Yüksektepe Ç., Soylu M.S., Saracoğlu H. et al. // Acta Crystallogr. – 2005. – **E61**. – P. o1158. – o1160.
21. Arslan H., Algül O. // Int. J. Mol. Sci. – 2007. – **8**. – P. 760. – 779.
22. Siddiqui S.A., Dwivedi A., Singh P.K. et al. // J. Struc. Chem. – 2009. – **50**. – P. 411. – 420.
23. Sundaraganesan N., Kumar K.S., Meganathan C. et al. // Spectrochim. Acta. – 2006. – **A65**. – P. 1186. – 1196.
24. Krishnakumar V., Ramasamy R. // Spectrochim. Acta . – 2005. – **A62**. – P. 570.
25. Weiqun Z., Baolong L., Yang C. et al. // J. Mol. Struct. (Theochem). – 2005. – **715**. – P. 117. – 124.
26. Scrocco E., Tomasi J. // Adv. Quant. Chem. – 1979. – **11**. – P. 115. – 121.
27. Luque F.J., Lopez J.M., Orozco M. // Theor. Chem. Acc. – 2000. – **103**. – P. 343. – 345.
28. Okulik N., Jubert A.H. // Internet Electron. J. Mol. Des. – 2005. – **4**. – P. 17.
29. Politzer P., Laurence P.R., Jayasuriya K. in: McKinney J. (Ed.), Structure Activity Correlation in Mechanism Studies and Predictive Toxicology, Special issue of Environ. Health Perspect. – 1985. – **61**. – P. 191.
30. Scrocco E., Tomasi J. Topics in Current Chemistry, Springer, Berlin, Vol. 7, 95. – 1973.
31. Politzer P., Truhlar D.G. Chemical Applications of Atomic and Molecular Electrostatic Potentials, Plenum, New York, 1981.
32. Kurtaran R., Odabasoğlu S., Azizoğlu A. et al. // Polyhedron. – 2007. – **26**. – P. 5069. – 5074.